

Space Photovoltaic Concentrator Using Robust Fresnel Lenses, 4-Junction Cells, Graphene Radiators, and Articulating Receivers

Henry W. Brandhorst, Jr.¹, Mark J. O'Neill², and A. J. McDaniel²

¹Carbpm-Free Energy, LLC, Auburn, AL USA, ² Mark O'Neill, LLC, Keller, TX 76248 USA

Brian Spence³ and Peter LaCorte³

³Deployable Space Systems, Inc., Goleta, CA 93117 USA

Paul Sharps⁴, Clay McPheeters⁴, Jeff Steinfeldt⁴

⁴SolAero Technologies, Albuquerque, NM 87123 USA

Michael Piszczor⁵ and Matt Myers⁵

⁵NASA Glenn Research Center, Cleveland, OH USA

Abstract

At the 42nd PVSC, recent advances in our space photovoltaic concentrator technology were presented. These advances include more robust Fresnel lenses for optical concentration, more thermally conductive graphene radiators for waste heat rejection, improved color-mixing lens technology to minimize chromatic aberration losses with 4-junction solar cells, and an articulating photovoltaic receiver enabling single-axis sun-tracking, while maintaining a sharp focal line despite large beta angles of incidence. In the past two years, under a NASA Phase II SBIR program, much additional progress has been made in the development of this new space photovoltaic concentrator technology, as described in this paper. New results include improved lens reinforcements, better lens articulation and updated mass values for the blanket assembly.

I. Introduction

As discussed at the 42nd PVSC, the TacSat 4 flight experiment (2011-2012) included one stretched linear Fresnel lens focusing sunlight at 8.5X geometric concentration ratio (8.5 cm wide lens) onto three series-connected Emcore ATJM cells (1.0 cm active width) assembled into a fully encapsulated dielectrically isolated photovoltaic receiver with a single 500 micron thick CMG cover glass over the receiver (about 11 cm long). Over the first six months of the mission, the power degradation of this photovoltaic concentrator unit was only 13% compared to 30% for neighboring Emcore (now SolAero) BTJM one-sun cells under 150 micron thick CMG cover glass, as expected¹. But, between the seventh month and the thirteenth month of the flight, the weak pre-tensioned silicone lens material suffered a mechanical failure after radiation embrittlement led to higher tear stress and lower tear strength². Since this failure, our team has developed far more robust lenses and made significant improvements in all areas for the Fresnel lens photovoltaic concentrator technology. This paper summarizes technology advances over the past two years, since our previous PVSC paper³.

Since May 2015, our team has been working under a NASA Phase II SBIR contract to develop a new photovoltaic concentrator including the following three key elements:

- A robust flat Fresnel lens comprising 100-micron tall silicone prisms (DC 93-500) molded onto either (1) a 50-micron thick ceria-doped glass superstrate, or (2) a mesh-reinforced 50-micron thick silicone base layer.
- 4-junction inverted metamorphic (IMM) solar cells with robust radiation shielding on both sides.
- Ultra-thin graphene sheet waste-heat radiator with coating to enhance emittance.

A critical development to permit articulation of the lens over beta angles up to 50° that enables the concentrator system to be used in single-axis sun-tracking arrays is presented. In addition, new rapid thermal test results for improved lens strengthening material using electroformed metal meshes over temperature ranges from -175C to +125C will be provided. Updated module

¹ President, AIAA Associate Fellow

² President

³ Chief Engineer

mass distributions will be presented. Additionally, new indoor simulator tests and projected AM0 testing using NASA's high altitude aircraft test facilities will be presented.

II. New Baseline Concentrator Module

To minimize the parts-count and to enable later mass-production of the new concentrator technology, our team has selected a baseline concentrator module, shown in Fig. 1, as the basic building block of the new array. The size of the optical element was selected to match the largest available size for a 50-micron thick toughened ceria-doped microsheet glass superstrate. The silicone (Dow Corning DC93-500) prisms are molded onto the inner surface of the glass superstrate to form two side-by-side linear Fresnel lenses. An alternate embodiment is to eliminate the glass and insert a metal mesh into the silicone for strength and stability (patent pending). The triangular prisms have a maximum height of 100 microns, with a mass-effective thickness of only 50 microns since the prisms only fill up half the volume of the prismatic pattern layer thickness (the other half is void).

The two lenses produce two focal lines on two photovoltaic receivers, each employing three 4-junction IMM cells. The lens aperture (5 cm) is 4X wider than the cell active width (1.25 cm), to enable $\pm 2^\circ$ sun-pointing tolerance in the critical lateral (alpha) direction and $\pm 50^\circ$ in the longitudinal (beta) direction. The 5 cm lens aperture width was selected before the potential of graphene radiators was known. This material is 5X better than carbon fiber reinforced composite sheet and 10X better than aluminum at spreading the waste heat over the radiator area. The next generation of this linear concentrator would use a larger lens aperture (e.g., 10 cm wide). The photovoltaic receivers are mounted onto 25-micron thick graphene sheet radiators for spreading and radiating the waste heat from the photovoltaic cells. The sheet is coated with silicone to increase emissivity.

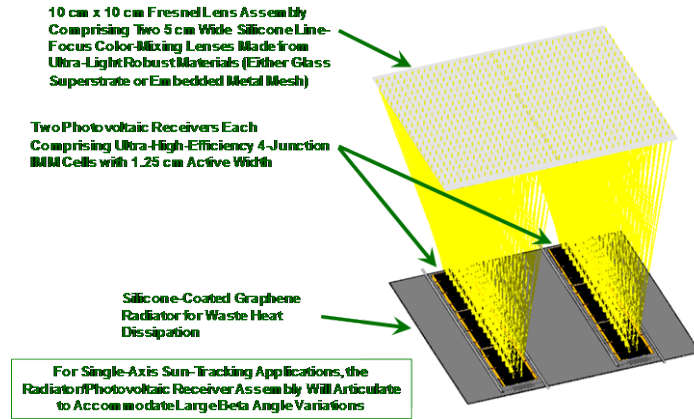


Figure 1. New baseline concentrator module

The next generation of this linear concentrator would use a larger lens aperture (e.g., 10 cm wide). The photovoltaic receivers are mounted onto 25-micron thick graphene sheet radiators for spreading and radiating the waste heat from the photovoltaic cells. The sheet is coated with silicone to increase emissivity.

The lenses are specially designed and optimized to focus well despite large variations in beta angle, by employing a small articulation of the receivers relative to the lens. Tests of this approach show that at 50° beta angle the focal lines are sharp and centered on the cells as shown in Fig. 2. The fixture employed to demonstrate this concept has a simple bar-linkage rotation. This fixture allows confirmation of the sharp line focus at the relevant beta angles from

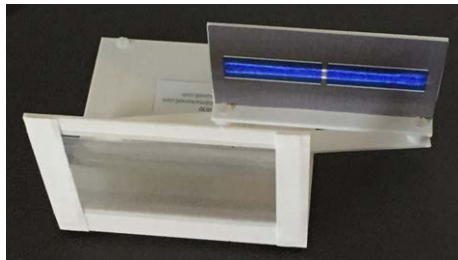


Figure 2. Focal line for 50° beta angle

0° to 50° . Quantitative testing of this novel approach is discussed in Section VI below.

III. 4-Junction Cells and Receivers

The prismatic pattern of the new lens is optimized to provide exceptional color-mixing to avoid chromatic aberration losses in the 4-junction IMM cells used in the new concentrator module. Fig. 3 shows one of the three-cell circuits produced for the new concentrator module. Each cell has a length of 3.2 cm and a total width of 1.5 cm. The three cells are wired in parallel with a single bypass diode protecting the three-cell group. The cell string is slightly shorter than the 10-cm focal line produced by the lens. The tabbing and interconnection scheme provides a robust assembly for ground testing. Flight units will be narrower and lighter. The 4-junction IMM cells are supported on glass carriers beneath the cells. This program is the first to use 4-junction IMM cells in a space concentrator application.



Figure 3. 4-junction IMM cell receiver

IV. Graphene Radiator Development

To decrease mass and increase thermal performance of the radiator, thin graphene sheets have been employed (patent pending). Graphene sheet offers a thermal conductivity to density ratio 10X better than aluminum sheet, and 5X better than carbon-fiber-reinforced sheet, and a 25-micron thickness is more than adequate for the concentrator module size shown in Fig. 1. Fig. 4 shows the thermal performance of a silicone-coated graphene radiator on GEO. The emittance of raw graphene is only 33% which is not acceptable. This shortcoming was solved by adding a silicone layer to increase the emissivity to an acceptable 70%. Note in Fig. 4 that the peak radiator temperature below the solar cell is less than 62C at GEO.

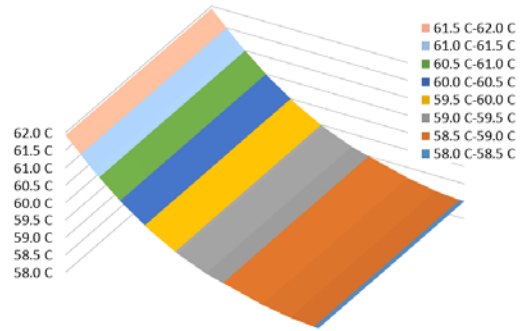


Figure 4. Graphene radiator thermal analysis

V. Improved Lens Material Approaches

Because of the lens damage noted in the TacSat 4 flight, two different ways of strengthening the lens have been developed over the past 5 years. The first approach uses a glass superstrate with silicone prisms molded onto the glass. The second approach uses a silicone lens with embedded mesh such as aluminum or stainless steel. Such a lens will of course employ a UV-rejection coating on the sun-exposed surface, as have the non-glass-superstrate lenses for several successful flight experiments (including the silicone mini-dome lenses on PASP+ in 1994-1995, the 4-year-exposed MISSE UVR-coated silicone samples on ISS, the UVR-coated stretched lens on TacSat 4), as well as in many ground tests. Previous radiation testing of these lenses with $5E12$ p+/cm² of 2.7 MeV protons showed no measurable change in transmittance. Recently, low energy (30 keV) proton testing to a dose of $1E16$ p+/cm² were conducted. Slight darkening was observed at this highest dose. The transmittance results are shown in Fig. 5. Because these test samples were uncoated, it is expected that a thin UV rejection coating would extend the hardness of these lenses.

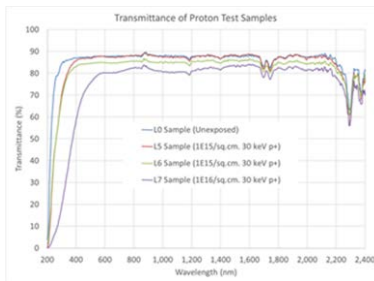


Figure 5. Spectral transmittance of 30 keV p+ irradiated samples

The second issue to be resolved with the new lens design is their ability to withstand thermal cycles. Accordingly, a sample with embedded electroformed stainless steel mesh was exposed to 2,000 rapid thermal cycles. The conditions were -175V to +125C for 516 cycles then -160C to +125C for 1484 cycles (to allow the test to be completed on schedule). Although the sample was supposed to be mounted in a stress-free manner, movement of the parts during the first cycle required more taping of the sample. In turn this led to some curling as seen in Fig. 6. Importantly, no tears were visible in the silicone, confirming the validity of this manner of reinforcement. It is believed that pinning of the corners and capturing the edges in loose slots would mitigate the observed curling. This strengthening approach saves mass and makes the lens assembly more robust.

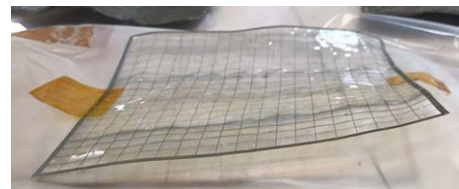


Figure 6. Stainless steel reinforced lens after 2,000 thermal cycles

VI. Lens Optical Performance Measurements at Different Beta Angles with IMM Cells in Articulating Receivers

One of the key innovative technologies being developed and demonstrated is the use of articulating photovoltaic receivers to accommodate large non-zero beta angles (longitudinal solar ray angles of incidence) to enable the new concentrator array to be deployed and supported on single-axis sun-tracking platforms (U.S. Patent No. 9,660,123). Recently a series of outdoor tests to measure the lens optical efficiency for various beta angles from zero to $\pm 50^\circ$ were conducted with the apparatus shown in Fig. 7. These tests were conducted for a nominal articulation path based on analytical and visual results.

A motorized polar-mount telescope tracker continuously aims the test article toward the sun. Two single-cell receivers are located in the focal lines of two lenses which were molded directly onto a single piece of ceria-doped

microsheet glass. The cells are mounted to an aluminum sheet heat sink, which is movable through a nominal U-shaped articulation path for different beta angles from -50° to $+50^\circ$. At each 10° increment in beta angle, the articulation path can be varied to determine if the nominal path is indeed the best path. The short-circuit current of the cell under test is used to measure the lens optical performance. For each data point, three different short-circuit currents are measured for the cell under test:

1. With the lens in place focusing onto the cell.
2. With the cell moved in front of the lens exposed to total (direct and diffuse) solar irradiance.
3. With the cell moved in front of the lens exposed only to diffuse solar irradiance by blocking the direct solar irradiance.

The difference between the second and third current measurements represents the one-sun current due to direct solar irradiance alone. Since the lens can only focus the direct solar irradiance, the ratio of the first current measurement to the difference between the second and third current measurements provides the **net concentration ratio** for the test. The **geometric concentration ratio** of the prototype concentrator equals the aperture width of each lens (5 cm) divided by the active width of each cell (1.4 cm) = 3.57X, slightly lower than the nominal design value of 4X. The prototype cells are 1.5 cm in total width but the bus bar and the tabs reduce the active width by 7% to 1.4 cm. The lens net optical efficiency is the ratio of net concentration ratio to geometric concentration ratio.

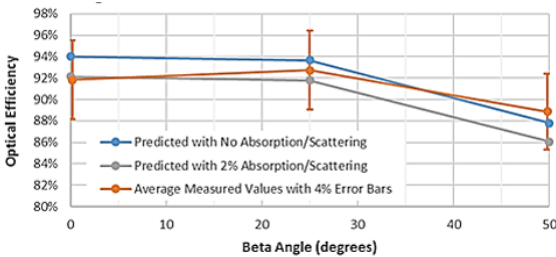


Figure 8. Measured and predicted net lens optical efficiency versus beta angle in outdoor testing

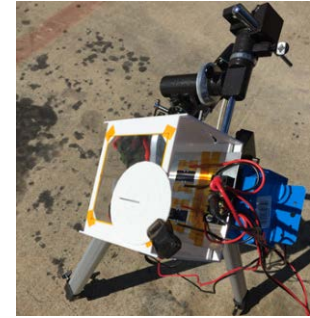


Figure 7. Apparatus for beta angle testing

The nominal articulation path was found to be the best path. Fig. 8 shows the measured net lens optical efficiency versus beta angle for the nominal receiver articulation path, and compares the measured results to predicted results. Two predicted curves are shown, the higher with zero absorption/scattering loss and the lower with 2% absorption/scattering loss (more realistic). The experimental data are shown with $\pm 4\%$ error bars, a rough estimate of the probable error in these measurements. Note the greatly expanded non-zero vertical axis in the graph. The predicted and measured results show excellent agreement.

VII. Updated Mass and Performance Metrics

A refined areal mass density estimate for the three key concentrator blanket elements is shown in Table 1. These key elements are the lens, heavily shielded photovoltaic receiver (150-micron equivalent cover glass front and back), and graphene radiator. An estimate the remaining array mass elements for the complete solar array wing, including the solar array deployment and support platform being developed by Deployable Space Systems using their patented roll-out solar array approach⁴ will be forthcoming. For the three limited elements shown in Table 1, the total areal mass density is about **0.399 kg/m²**. While there will be additional mass and additional power losses for a full array, a very simplistic calculation using a future cell efficiency of 39% at 4X (equivalent to 35% at 1 sun), a lens optical efficiency of 90%, and the areal mass density of 0.399 kg/m² for these three concentrator blanket

Table 1. Mass breakdown of lens, photovoltaic receiver assembly & radiator for the updated 4X concentrator blanket

Geometric Concentration Ratio		4.00 X	Physical Concentration Ratio			3.03 X
Aperture Width		5.00 cm	Cell Width	1.45 cm	Receiver Width	1.65 cm
Major Subsystem	Element	Element Area per sq.m. Aperture	Thickness	Density	Mass/ Aperture	Subtotals: Mass/Aperture
		(sq.m.)	(cm)	(g/cu.cm.)	(kg/sq.m.)	(kg/sq.m.)
Lens	Silicone	0.90	0.010	1.030	0.093	0.133
	Stainless Mesh	0.10	0.005	8.000	0.040	
Radiator	Silicone	1.000	0.005	1.030	0.052	0.102
	Graphene	1.000	0.003	2.000	0.050	
Receiver	CMG Microsheet Cover Glass	0.330	0.008	2.550	0.083	0.165
	Cover Glass Adhesive	0.330	0.003	1.030	0.009	
	IMM Cell	0.330	0.001	5.300	0.017	
	Glass Carrier	0.330	0.008	2.550	0.083	
	Thermally Conductive Adhesive	0.330	0.003	1.500	0.012	
Totals					Specific Power	Areal Mass Density
Dual Blanket Concentrator for 35% Cell at One-Sun (39% Cell at Concentration)					1.202 W/kg	0.399 kg/sq.m.
Equivalently Shielded One-Sun Blanket for 35% Cell					652 W/kg	0.733 kg/sq.m.

elements alone yields a specific power of 1,200 W/kg, as shown in Table 1. A similar simplistic analysis for an equally shielded one-sun cell blanket yields 650 W/kg, as also shown in Table 1.

Compared to a conventional one-sun space array, the new concentrator uses about 75% less of the expensive IMM cell area to produce each watt of power in space. Because the remaining concentrator blanket materials (glass, silicone, graphene, etc.) are relatively reasonable in cost, a realistic target cost for the new concentrator array is at least **50% lower** than for a one-sun array of the same power rating.

VIII. AM0 Testing of Concentrator Module

Outdoor testing of concentrator modules on clear days can be easily accomplished as noted above, but the solar spectrum of the test does not simulate outer space sunlight. Obtaining accurate AM0 performance data for concentrator arrays with terrestrial simulators is difficult under the best of conditions. Key issues include the need to closely match the AM0 spectrum for the 4 junction IMM cell, and the need for excellent collimation of the incident light for the concentrator lens to focus properly. The best measured results of the concentrator module are shown in Fig. 9. There was both lateral and longitudinal misalignment of beam to concentrator cell and the spectral match was not perfect. Although neither of the required conditions was completely achieved the results

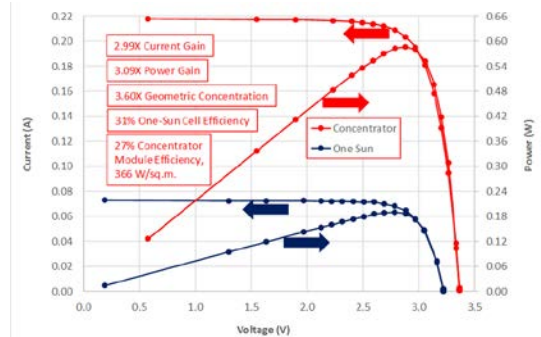


Figure 9. LAPSS performance test results

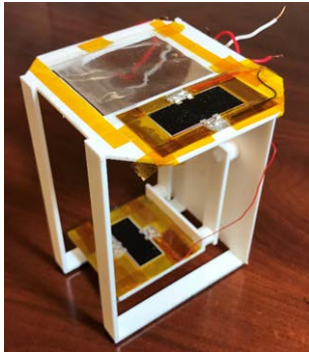


Figure 9. Concentrator module for near-AM0 testing

were encouraging. Thus, both the terrestrial outdoor testing and indoor simulator results were encouraging, more accurate results are desired.

Hence a third approach is planned for the future to obtain accurate performance data using near-AM0 testing using NASA's high altitude aircraft test facilities. Therefore, the concentrator module tested at SolAero was configured to fit within NASA's aircraft test facilities, as shown in Fig. 10. The concentrator cell is aligned below the reinforced lens that is 5.0 cm wide and 4.0 cm long. The 4X concentrator cell is 1.25 cm wide and 3.2 cm long. There is an additional 1-sun test cell at the top of the fixture to provide comparative one-sun cell performance. The module is designed to fit within the 11-cm diameter collimating tube on the airplane. The unit has a height of 11 cm. The NASA aircraft test facility flies at altitudes up to 50,000 feet and can orient the test solar cell assembly to the sun with an accuracy of 1° or better. Data are taken as the flight descends and the results taken above the tropopause are extrapolated to AM0. A correction for ozone absorption above 50,000 feet is also applied. It is

believed that these results will have an error less than 2%. Since the module has already been tested at SolAero, direct comparison of measurements will be possible.

Acknowledgments

The work reported in this paper was made possible by a NASA Phase II SBIR contract from NASA GRC to Mark O'Neill, LLC. Our team is grateful to NASA for supporting this work. We are also grateful to Dr. Scott Messenger previously of SRM Consulting and Dr. Dave Wilt of the Air Force Research Lab (AFRL) for their important contributions in radiation testing and optical property measurements, respectively.

References

- ¹P. Jenkins et al., "Initial Results from the TacSat-4 Solar Cell Experiment," *39th IEEE PVSC*, 2013.
- ²M. O'Neill et al., "Development of More Robust Stretched Lens Array (SLA) Technology with Improved Performance Metrics and Significantly Expanded Applications," *23rd Space Photovoltaic Research and Technology (SPRAT) Conference*, 2014.
- ³M. O'Neill et al., "Recent Space PV Concentrator Advances: More Robust, Lighter, and Easier to Track," *42nd IEEE PVSC*, New Orleans, 2015.
- ⁴B. Spence et al., "Rollable and Accordion Foldable Refractive Concentrator Space Solar Array Panel, *U.S. Patent 8,636,253*, 2014.